

# UC San Diego

## UC San Diego Previously Published Works

### Title

Computational Evidence for Underweighting of Current Error and Overestimation of Future Error in Anxious Individuals

### Permalink

<https://escholarship.org/uc/item/4334k3tb>

### Journal

Biological Psychiatry Cognitive Neuroscience and Neuroimaging, 5(4)

### ISSN

2451-9022

### Authors

Howlett, Jonathon R  
Thompson, Wesley K  
Paulus, Martin P

### Publication Date

2020-04-01

### DOI

10.1016/j.bpsc.2019.12.011

Peer reviewed



# HHS Public Access

Author manuscript

*Biol Psychiatry Cogn Neurosci Neuroimaging*. Author manuscript; available in PMC 2021 April 01.

Published in final edited form as:

*Biol Psychiatry Cogn Neurosci Neuroimaging*. 2020 April ; 5(4): 412–419. doi:10.1016/j.bpsc.2019.12.011.

## Computational Evidence for Underweighting of Current Error and Overestimation of Future Error in Anxious Individuals

Jonathon R. Howlett<sup>1,2,\*</sup>, Wesley K. Thompson<sup>2,3</sup>, Martin P. Paulus<sup>1,2</sup>

<sup>1</sup>Department of Psychiatry, University of California San Diego, La Jolla, CA, USA

<sup>2</sup>Laureate Institute for Brain Research, Tulsa, OK, USA

<sup>3</sup>Department of Family Medicine and Public Health, University of California San Diego, La Jolla, CA, USA

### Abstract

**Background:** Real-time control of goal-directed actions requires continuous adjustments in response both to current error (i.e. distance from goal state) and predicted future error. Proportion-integral-derivative (PID) control models, which are extensively used in the automated control of industrial processes, formalize this intuition. Previous computational approaches to anxiety have separately addressed behavioral inhibition and exaggerated error processing, but a PID control approach decomposing error processing into current and anticipated error could integrate these accounts and extend them to a real-time sensorimotor control domain.

**Methods:** We applied a simplified proportion-derivative (PD) control model to a virtual driving task in a transdiagnostic psychiatric sample of 317 individuals and computed a drive parameter (weighting of current error) and a damping parameter (weighting of the rate of change of error, enabling adjustment based on future error).

**Results:** Self-reported fear but not negative affect was selectively associated with lower drive and lower damping. Those individuals that were characterized by lower drive and damping also exhibited lower caudal anterior cingulate cortex (ACC) but not insula volume in a structural MRI analysis.

**Conclusions:** Taken together, the PD control approach reveals that fear is specifically associated with reduced weighting of current error and overestimation of future error, resulting in both approach inhibition and in overcorrecting overshoots around a goal state.

\*Corresponding Author: Jonathon R. Howlett, MD, University of California San Diego, Department of Psychiatry, 9500 Gilman Dr, La Jolla, CA 92093, jhowlett@ucsd.edu.

The Tulsa 1000 Investigators include the following contributors: Robin Aupperle, Ph.D., Jerzy Bodurka, Ph.D., Yoon-Hee Cha, M.D., Justin Feinstein, Ph.D., Sahib S. Khalsa, M.D., Ph.D., Rayus Kuplicki, Ph.D., Martin P. Paulus, M.D., Jonathan Savitz, Ph.D., Teresa A. Victor, Ph.D.

**Publisher's Disclaimer:** This is a PDF file of an unedited manuscript that has been accepted for publication. As a service to our customers we are providing this early version of the manuscript. The manuscript will undergo copyediting, typesetting, and review of the resulting proof before it is published in its final form. Please note that during the production process errors may be discovered which could affect the content, and all legal disclaimers that apply to the journal pertain.

## Keywords

Anxiety; Computational Psychiatry; Motor Control; Anterior Cingulate Cortex; Bayesian Models; Negative Affect

---

## Introduction

In pursuing our goals, we must continuously make adjustments based on errors, i.e. the difference between where we are and where we would like to be. These adjustments must be based not only on the current situation (i.e. current error), but also on how we expect the situation to evolve (anticipated future error). Without this capacity to extrapolate a trajectory into the future and adjust our behavior accordingly, vigorous goal pursuit can result in a series of overcorrecting overshoots around the goal state. The development of techniques to solve this problem was a major advance in the automated control of industrial processes (1). Individuals must solve an equivalent problem when pursuing real-time control of goal-directed actions and a deficit in this fundamental process could be related not only to gross abnormalities in the motor system but also to higher level cognitive and affective processing dysfunctions. Individuals with high trait anxiety were found to have difficulty selecting optimal actions when adjusting to the temporal statistics of the environment (2). Moreover, anxiety has been linked to exaggerated error signaling in the dorsal anterior cingulate cortex (dACC) (3). Some researchers have argued that behavioral inhibition is a central aspect of anxiety (4), suggesting that anxious individuals may exhibit an attenuated drive to reach a goal in addition to an inability to avoid overcorrecting overshoots around a goal. A control-theoretic account of behavioral adjustments as a function of real-time error magnitude could therefore elucidate fundamental anxiety-related processing dysfunctions. This can be accomplished through the use of a proportion-integral-derivative (PID) control modeling approach.

PID controllers are the most widely used controllers in industrial systems today and were originally developed in 1922 as a model of steering by human ship pilots (5). In PID control, the control action is a linear combination of three terms that capture current, past, and future error: (1) the proportion term is the weighted *current error* (difference between goal state and current state), (2) the integral term is the weighted integral of the error over time (i.e. *past error*), and (3) the derivative term is the weighted derivative (rate of change) of the error (enabling adjustment based on anticipated *future error*). The combination of these terms allows for rapid correction of errors (i.e. goal pursuit) while minimizing overcorrection (which results in large overshoots around the goal state). The coefficients or weighting factors for the three terms,  $K_p$ ,  $K_i$ , and  $K_d$ , are known as gains.  $K_p$  is a *driving* parameter that controls propulsion toward the goal based on current error and influences the *rise time*, or time to initially reach the goal state.  $K_d$  is a *damping* parameter, analogous to friction in a physical system, that minimizes overcorrection by anticipating future error and thereby influences the *settling time*, or the time until oscillations around the goal state fall within a certain small range. Higher  $K_d$  (i.e. damping) is necessary in the setting of higher  $K_p$  (i.e. drive), with the combination helping to mitigate the inherent tradeoff between fast rise time and fast settling time.  $K_i$  is a parameter that responds to past error over time and thereby

eliminates residual steady-state error resulting from a constant disturbance such as gravity.  $K_p$ ,  $K_i$ , and  $K_d$ , are typically tuned heuristically rather than optimizing based on a mathematical model of the system. The origins of PID as a model of human control performance underline its potential value as an approach to real-time behavioral adjustments in humans. PID control has been successfully applied to human motor performance in terms of balance (6, 7), simulated control of the forearm (8), and skilled operation of machinery (9). A PID modeling approach could help refine accounts of error processing in anxious individuals by separately examining the weighting of current error and anticipated future error. If these individuals underweight current error, while also underweighting the rate of decrease in error (thus overestimating future error), this would lead to behavior that is both under-driven and under-damped, consistent with a combination of behavioral inhibition and overcorrecting overshoots around the goal. This would argue for an account of anxiety as involving a fundamental deficit in error prediction.

In 2010, the National Institute of Mental Health (NIMH) initiated the Research Domain Criteria (RDoC) framework, which aims to integrate information across multiple units of analysis to develop a dimensional, neuroscience-based psychiatric classification system (10). RDoC is organized into domains of functioning, with the negative valence domain being the most broadly relevant to anxiety disorders. Within the negative valence domain, the construct of fear, or response to an acute threat, can be distinguished from negative affect or distress more generally, and has good convergent and discriminant validity on self-report measures (11). This distinction between fear and broader negative affect has critical implications for the assessment and treatment of individuals with anxiety-related complaints, as variability in levels of fear is observed both between and within anxiety-related diagnostic categories (12). Fear is behaviorally associated with increased avoidance behaviors, decreased approach behaviors, and response inhibition. Physiologically, fear is accompanied by autonomic arousal and increased startle response (13). A closely related construct is anxious arousal, which has been distinguished from anxious apprehension in characterizing two separate factors cutting across multiple anxiety-related disorders (14). Importantly, a new sensorimotor domain has recently been added to the RDoC framework (15), reflecting a growing awareness that new models relating negative valence processing to alterations in real-time motor behavior may hold great promise in refining our understanding of processing dysfunctions in anxiety disorders.

We examined the relationship between self-reported fear and performance on a task in which subjects controlled a virtual car via a joystick (16). Because the combination of inhibited approach behavior (4) and exaggerated error processing (3) suggest that fear may be associated with motor behavior that is both under-driven and under-damped, we hypothesized that fear would be associated with lower  $K_p$  and  $K_d$ . We further hypothesized that low  $K_p$  and  $K_d$  would be associated with lower brain volumes in two regions that are closely associated with fear, the insula and the dorsal anterior cingulate cortex (dACC) (13). The dACC in particular is associated with error monitoring (3) and fear expression (17) and is believed to be key region through which affective state influences motor control processes (18). Consistent with the National Institute of Mental Health Research Domain Criteria (RDoC) (10) approach, our sample consisted of a combination of healthy volunteers and a transdiagnostic group consisting of individuals with anxiety and mood problems.

In industrial applications, PD and PI controllers (as opposed to full PID controllers) are common. Here we use a PD rather than a full PID model for three reasons: (1) We hypothesized that fear would be related to differences in  $K_p$  and  $K_d$  rather than  $K_i$ . (2) Our task design does not include a constant disturbance, and therefore  $K_i$  is not necessary to eliminate steady-state error. (3) The integral of error is expected to correlate with current error, presenting difficulties for model-fitting if both  $K_p$  and  $K_i$  were included.

## Methods and Materials

All study procedures were approved by the Western Institutional Review Board, and all participants provided written informed consent prior to participation.

### Participants

The experiment was performed as part of the Tulsa-1000 (T-1000) study, which is aimed at multilevel assessment and outcome prediction in a large, heterogeneous psychiatric sample. Subjects were recruited from mental health providers or via advertisements. At screening, treatment-seeking individuals were required to have a score on the Patient Health Questionnaire-9 (PHQ-9)  $\geq 10$  and/or on the Overall Anxiety Severity and Impairment Scale (OASIS)  $\geq 8$  (cutoff scores were based on the validation studies for these measures (19, 20)). 317 subjects (age:  $35.42 \pm 11.35$  years; gender: 104 male and 213 female) participated in the experiment, of whom 259 were in the mood/anxiety group and 58 in the healthy control group. Psychiatric diagnoses based on the MINI Neuropsychiatric Interview (MINI) (21) are shown in Supplementary Table S1, with additional demographic and clinical information shown in Supplementary Table S2.

### Experiment

Subjects performed a simulated one-dimensional driving task (Figure 1) (16). The position of a virtual car was controlled using a gaming joystick. Each subject completed 30 trials. In each trial, subjects were instructed to drive the car as quickly as possible and stop as close as possible to a stop sign without crossing the stop-line. Each trial had a fixed duration of 10 seconds. The car was controlled according to a linear dynamical system, in which car velocity was proportional to joystick displacement. Throughout each trial, continuous joystick displacement was recorded with a sampling window of 1/60 second. In order to assess affective state including fear and general negative affect, participants completed the Positive and Negative Affect Schedule-Expanded Form (PANAS X) (22). The PANAS X is a hierarchical self-report measure of emotional states which includes two higher order dimensions (Positive Affect and Negative Affect) as well as 11 specific affects: Fear, Sadness, Guilt, Hostility, Shyness, Fatigue, Surprise, Joviality, Self-Assurance, Attentiveness, and Serenity. Both the higher order dimensions and specific affect scales have demonstrated high internal consistency, test-retest reliability, and convergent and discriminant validity (22). Participants completed the trait version of the PANAS X, with instructions asking “How do you feel in general?”

## Behavioral Analysis

We plotted the log of mean speed throughout the course of the 10-second trial to visualize individual differences in behavioral performance. This was calculated as the log of the mean of the absolute value of velocity across all trials for each subject, and captures both rise time (with fast rise time corresponding to higher speeds early in the trial) and settling time (with fast settling time, meaning less pronounced oscillations, corresponding to lower speeds later in the trial). To quantify the relationship between self-reported fear and log mean speed, we performed a linear regression analysis at each sampled time point, controlling for gender, age, and education. To investigate the relationship between gender and log mean speed, we performed an otherwise identical analysis controlling for age and education

## PD Control Model

We performed hierarchical Bayesian estimation of PD model parameters using the Rstan (23) interface to the Stan (24) language (Figure 1, Figure 2, and Supplementary Figure S1). At each time point within a trial, acceleration was modeled as a linear combination of current error (goal position minus current care position) and derivative of the error, with coefficients  $K_p$  and  $K_d$ , respectively. In turn,  $K_p$  and  $K_d$  for each trial were modeled as being drawn from subject-level distributions. Finally, these subject-level means were modeled as being drawn from overall group-level distributions, while also potentially depending on subject-level predictors (gender, age, and self-reported affect). See Supplementary Methods for further modeling details.

## Fear and Model Parameters

To determine the relationship between fear and model parameters, we constructed a hierarchical model in which both the subject-level mean  $K_p$  and the subject-level mean  $K_d$  depended on scaled (i.e. z-scored) age, gender, and PANAS X Fear. Effect sizes for the relationships between subject-level predictors and subject-level  $K_p$  and  $K_d$  were calculated by dividing each draw of the posterior distribution of the slope by the posterior distribution of the standard deviation of subject-level  $K_p$  and  $K_d$ . This yielded the equivalent of a standardized regression coefficient or beta weight, i.e. an estimate of the change (in standard deviations) of the dependent variable per standard deviation of the predictor variable.

To test the specific effect of fear as distinguished from negative affect more generally, we constructed a model otherwise identical to the above, but adding PANAS X Negative Affect score as an additional predictor of subject-level mean  $K_p$  and  $K_d$ .

## Brain Volumes and Model Parameters

In order to test the relationship between model parameters and brain volumes, 302 subjects completed structural MRI scans. Volumes of individual brain regions were obtained using FreeSurfer (see Supplementary Methods section for details). Two brain regions were selected as *a priori* regions of interest: caudal ACC and insula. For each brain region, we first calculated the mean of the left and right volume for each subject. We then constructed two hierarchical models: in each model, both the subject-level mean  $K_p$  and the subject-level mean  $K_d$  depended on the scaled volume of the region of interest, in addition to total cortical volume, gender, and age.

## Results

### Behavioral Results

The relationship between self-reported fear and log mean speed at each time point during the trial, controlling for gender, age, and education is shown in Figure 3a. Results demonstrate that individuals reporting high levels of fear displayed a lower speed early in the trial (corresponding to slow rise time) and a higher speed late in the trial (corresponding to slow settling time). The relationship between gender and log mean speed controlling for age and education is shown in Figure 3b. Males demonstrated a higher speed early in the trial (corresponding to fast rise time) and a lower speed late in the trial corresponding to fast settling time).

### Fear and Model Parameters

PANAS X Fear score was associated with lower  $K_p$  (median  $\beta = -0.12$ , 95% credible interval  $\beta = [-0.23, -0.01]$ , 1.9% of the posterior greater than zero; Supplementary Figure S7a) and lower  $K_d$  ( $\beta = -0.19 [-0.30, -0.07]$ , 0.1% of the posterior greater than zero; Figure 4a). Male gender was associated with higher  $K_p$  ( $\beta = 0.26 [0.15, 0.38]$ , 0.0% of the posterior less than zero) and higher  $K_d$  ( $\beta = 0.29 [0.18, 0.41]$ , 0.0% of the posterior less than zero). Older age was associated with lower  $K_p$  ( $\beta = -0.13 [-0.24, -0.01]$ , 1.4% of the posterior greater than zero) and lower  $K_d$  ( $\beta = -0.12 [-0.24, -0.00]$ , 2.3% of the posterior greater than zero). See Supplementary Figure S8 for plots of the relationship between PANAS X Fear and model parameters (extracted from the hierarchical model).

After controlling for negative affect, PANAS X Fear score remained associated with lower  $K_p$  ( $\beta = -0.27 [-0.50, -0.03]$ , 1.2% of the posterior greater than zero; Supplementary Figure S7b) and lower  $K_d$  ( $\beta = -0.25 [-0.50, -0.01]$ , 1.8% of the posterior greater than zero; Supplementary Figure S7c). There was no credible association between PANAS X Negative Affect score and  $K_p$  ( $\beta = 0.17 [-0.07, 0.40]$ , 8.2% of the posterior less than zero) or  $K_d$  ( $\beta = 0.07 [-0.17, 0.31]$ , 27.8% of the posterior less than zero).

### Brain Volumes and Model Parameters

Caudal ACC volume was associated with higher  $K_p$  ( $\beta = 0.20 [0.06, 0.34]$ , 0.3% of the posterior less than zero; Supplementary Figure S10) and higher  $K_d$  ( $\beta = 0.20 [0.06, 0.34]$ , 0.1% of the posterior less than zero; Figure 4b). Insula volume was not associated with  $K_p$  ( $\beta = -0.01 [-0.21, 0.18]$ , 45% of the posterior greater than zero) or  $K_d$  ( $\beta = -0.06 [-0.26, 0.13]$ , 26% of the posterior greater than zero).

## Discussion

This investigation used a virtual driving task using a PD control model with driving ( $K_p$ ) and damping ( $K_d$ ) parameters to examine whether individuals with high levels of fear show altered processing of current and future errors. There were three main results. First, individuals with higher levels of fear showed lower levels of both drive and damping even after controlling for negative affect. Although males had higher values for both drive and damping, and older individuals showed lower drive and damping, the associations between

fear and model parameters were present whether or not age and gender were included as covariates in the models. Second, in an a priori region-of-interest analysis, higher levels of drive and damping were associated with larger gray matter volume in the caudal ACC, after controlling for total cortical volume. Third, the reliability of estimating both  $K_p$  and  $K_d$  was high, which means that trial noise is small compared to the variance between subjects and that parameters can be estimated reliably even with a small number of trials per subject. Taken together, this approach shows that high fear individuals relative to low fear individuals show attenuated processing of current but an exaggerated processing of future errors during a motor task.

In our sensorimotor control task, individuals reporting high levels of fear do not overweight *current* error, but rather overestimate *future* error because of an underweighting of the error's rate of decrease (i.e. derivative). Thus, these individuals can simultaneously display inhibited approach behavior (i.e. slow rise time) due to low  $K_p$  and overcorrecting oscillations around the goal (i.e. slow settling time) due to low  $K_d$ . A PD control approach can thereby integrate behavioral inhibition and over-responsiveness to error within a unified modeling perspective. The combination of slower rise time with longer settling time demonstrates that fearful individuals are behaving suboptimally, rather than placing greater weight on speed or accuracy. The idea that fear is associated with exaggerated prediction of future error is consistent with a view of anxiety disorders as fundamentally involving altered anticipatory processing (25).

The need for computational approaches to explicitly model the role of brain processes in generating behavior, thus developing a more precise understanding of altered behavior in anxiety, has been increasingly recognized (26). Ideally, such approaches could disentangle fear, or response to an acute threat, from negative affect or distress more generally, a distinction with critical implications for the assessment and treatment of individuals with anxiety-related complaints (11, 12). Previous computational accounts have shed light on the quantitative mechanistic underpinnings of anxiety-related constructs. For example, Bayesian analysis has recently been applied to develop a normative framework for behavioral inhibition in approach/avoidance conflict scenarios (27). As expected, behavioral inhibition within this framework was positively associated with trait anxiety (27) and reduced by administration of a benzodiazepine (an anxiolytic medication) and by lesions of the amygdala (which is involved in fear learning and fear expression) (28). Another computational approach to anxiety is to characterize the scaling of error information based on environmental statistics. Adjustments to prediction errors (i.e. learning) should be sensitive to underlying environmental statistics, because an error in a volatile context is more likely to represent a true change, while an error in a stable context is more likely to represent noise. Anxious individuals have been shown to be poorer at adjusting response to error (known as the learning rate) based on environmental statistics (29), and to suboptimally display a higher "lose-shift" rate in a stable environment (30). As a result, these individuals can fail to settle into a stable behavioral pattern, and instead continue to over-adjust behavior in response to statistical noise.

One challenge facing a more integrative computational account of anxiety is to combine the two constructs discussed above, i.e. behavioral inhibition and over-responsiveness to error,



within a single framework. As noted above, behavioral inhibition has been largely analyzed within explicit approach/avoidance conflict scenarios such as foraging in the presence of a predator or approaching a potential social partner who may or may not be friendly. These conflict scenarios are clearly ubiquitous both in evolutionary history and in everyday life, and help explain key clinical aspects of anxiety disorders (31). However, suboptimal error scaling in anxious individuals is observed even in the absence of an explicit approach/avoidance conflict. Moreover, when adopting a simple but powerful control-theoretic conceptualization of error as the distance between the current state and a goal, greater error responsiveness would correspond to a *less* inhibited goal approach, the opposite of what is observed in anxiety. The PD control modeling approach can help resolve this paradox and extend computational accounts of anxiety into a real-time sensorimotor control domain by decomposing error processing into separate terms for current and anticipated error.

The specific relationship between PD model parameters and fear, even after controlling for other affects including general negative affect, suggests that this approach could provide a specific assessment for a subset of individuals with anxiety-related complaints, as opposed to those experiencing distress more generally. Even within individuals endorsing anxiety-related complaints, levels of fear (which includes an arousal component) vary both across and within anxiety-related diagnoses (12). It is therefore possible that the altered control performance observed in our paradigm is specifically associated with this arousal component, leading to a stronger relationship between model parameters and fear as opposed to negative affect or trait anxiety (see Supplementary Results). Model parameters which specifically relate to fear rather than negative affect more generally may allow assessment of a dimension which cuts across diagnostic lines while differentiating individuals within diagnostic categories, consistent with the goals of RDoC (10).

While fear is negatively associated with both  $K_p$  and  $K_d$ , the high correlation between these two parameters across subjects raises the question of whether they can be disambiguated in our paradigm. Furthermore, as shown in Supplementary Figure S1, velocity traces for a given  $K_p$  are relatively similar across the range of observed  $K_d$  values. Our results do provide some evidence that, despite the high correlation, we can successfully recover these parameters independently. Simulations and parameter recovery shows that the model can reliably recover these two parameters when they are generated independently (i.e. are uncorrelated). Simulations with correlated  $K_p$  and  $K_d$  also show that the model can reliably recover residual  $K_d$ , controlling for  $K_p$ . Split half reliability results also show that the model reliably recovers residual  $K_d$ , controlling for  $K_p$ , from real data. Partial correlations show that fear is negatively associated with  $K_d$ , controlling for  $K_p$ , but may be *positively* associated with  $K_p$ , controlling for  $K_d$ . This suggests that the negative relationship with  $K_d$  may be more fundamental, and that subjects with high fear may display inhibited approach because of a limited capacity for damping, although further research will be needed to test this causal hypothesis.

Much of the recent research on the computational mechanisms underlying human motor control has incorporated a different body of engineering techniques known as optimal control theory (32). Optimal control theory employs calculus of variations to minimize a chosen performance measure given a mathematical model of a system (33). The

performance measure must explicitly account for all competing goals relevant to a control policy (such as maximizing accuracy while minimizing energetic costs) and must explicitly weight the relative importance of each goal. While optimal control theory has proven to be a powerful approach to understanding the human motor system, it may not straightforwardly map onto suboptimal motor performance in psychiatric disorders. While it is unlikely that PID control will offer a full account of human motor performance, its simplicity, flexibility, and interpretability, especially with respect to suboptimal behavioral functioning such as slow responsiveness or large oscillations, suggest it may hold great utility for delineating individual differences in real-time behavioral control in psychiatric disorders. Optimal control and PD control may therefore represent complementary approaches to understanding the full range of human real-time behavioral control processes.

The ability to reliably measure individual behavioral differences, ideally with short testing sessions amenable for use in clinical populations, is critical for the growing field of computational psychiatry. Recent investigations have highlighted the challenge of this endeavor by demonstrating the poor individual-level reliability of an assortment of common behavioral paradigms. For example, common behavioral paradigms used to measure self-regulation have shown low test-retest reliability due to relatively low levels of between-subject variance compared to within-subject variance and error variance (34). In fact, many common behavioral tasks have been designed to exhibit a low between-subject variance, leading to robust task effects but a lack of reliability in measuring individual differences (35). Bayesian hierarchical modeling is an ideal approach to accurately characterize different sources of variance (36) and has demonstrated that high variability within-subject (i.e. trial noise) is a major impediment to reliably estimating individual differences in common inhibitory control paradigms, especially when the number of trials per subject is low (37). In contrast, our results indicate that, even at the level of a single trial, variance in  $K_p$  and  $K_d$  are more attributable to between-subject differences than within-subject differences (i.e. trial noise). The high level of between-subject variability and low level of trial noise indicates that subject-level parameters in our paradigm can be estimated with high reliability, even with a small number of trials per subject. These findings suggest that real-time sensorimotor paradigms could offer substantially improved reliability in measuring individual differences compared to common discrete decision-making or reaction time paradigms and thus may warrant far greater attention within computational psychiatry.

The advantages of the present approach include a simple data collection procedure and a hierarchical model-fitting process yielding highly reliable model parameters. Our generative model specifically predicts acceleration at each time-point during each trial and reliably captures individual behavioral differences on the task. The model parameters demonstrate a relationship to self-reported fear, demonstrating a link between high-level affective processing and real-time sensorimotor control. Crucially, there is a specific relationship to fear even after controlling for general negative affect as well as other specific affects, a distinction that may have critical clinical implications for delineating neural dysfunction in separate psychiatric sub-populations. The model parameters are also related to age and gender, as well as to volumes in the ACC, a region linked to fear, error processing, and motor control. The present study also has the advantage of a large, heterogeneous sample.

Limitations of the current study include the cross-sectional design, thus limiting insight into the relationship between changes in model parameters and changes in fear over time. Another limitation is the lack of fMRI data to examine the real-time neural mechanisms underlying the observed performance differences. Future research can also examine relationships between model parameters and other fear- and anxiety-related brain regions, such as the amygdala (which was not measured in our FreeSurfer cortical volume analysis). Another limitation is that, while our analyses were hypothesis-driven, our hypotheses were not pre-registered. The T1000 study includes a plan to conduct confirmatory replications in an independent sample with pre-registered hypotheses. Finally, an important limitation is the inability to fully separate state estimation from control in our paradigm. Because we are unable to directly infer the subject's estimate of the current state (which is influenced by sensory and motor noise), it is difficult to determine whether the observed differences in parameters between subjects could be accounted for in part by biased estimation of current position and velocity rather than different weightings placed on these estimates. Previous research employing an optimal feedback control framework to study limb movements has applied external perturbations to explicitly measure the motor response to an experimenter-controlled sensory input (38). A similar approach could help disambiguate state estimation from control in our paradigm.

In summary, we employed a PD control model to a sensorimotor control task and demonstrated that subjects reporting high levels of fear displayed decreased weighting on current error (consistent with inhibited goal approach) and also decreased weighting on the rate of change of error (leading to overcorrecting oscillations around the goal). These findings were specific to fear after controlling for general negative affect. This parameter pattern observed in subjects with high fear ratings was also observed in females, older subjects, and in subjects with lower volumes in the ACC. The results demonstrate that a fairly simple task paradigm can generate highly reliable, potentially clinically relevant parameters, and help extend and integrate prior computational analyses of anxiety into a real-time sensorimotor control domain.

## Supplementary Material

Refer to Web version on PubMed Central for supplementary material.

## Acknowledgments

This work has been supported in part by The William K. Warren Foundation and the National Institute of General Medical Sciences Center Grant Award Number 1P20GM121312. The content is solely the responsibility of the authors and does not necessarily represent the official views of the National Institutes of Health. The <http://ClinicalTrials.gov/identifier> for the clinical protocol associated with data published in the current paper is NCT02450240, "Latent Structure of Multi-level Assessments and Predictors of Outcomes in Psychiatric Disorders".

### Disclosures

Dr. Howlett previously received funds through his institution to participate in a clinical trial for a Janssen medication. Dr. Paulus is an advisor to Spring Care, Inc., a behavioral health startup, and has received royalties for an article about methamphetamine in Uptodate. Dr. Paulus is supported by a grant from the National Institute of Mental Health (R01 MH101453), from the National Institute on Drug Abuse (U01 DA041089) and National Institute of General Medical Sciences (P20GM121312). Dr. Thompson reports no biomedical financial interests or potential conflicts of interest.

## References

1. Johnson MA, Moradi MH (2005): PID control. Springer.
2. Browning M, Behrens TE, Jochem G, O'Reilly JX, Bishop SJ (2015): Anxious individuals have difficulty learning the causal statistics of aversive environments. *Nat Neurosci.* 18:590–596. [PubMed: 25730669]
3. Hajcak G, Foti D (2008): Errors are aversive: defensive motivation and the error-related negativity. *Psychol Sci.* 19:103–108. [PubMed: 18271855]
4. Gray JA (1982): *The neuropsychology of anxiety: An enquiry into the functions of the septo-hippocampal system.* New York, NY: Oxford University Press.
5. Minorsky N (1922): Directional stability of automatically steered bodies. *Journal of the American Society for Naval Engineers.* 34:280–309.
6. Hidenori K, Jiang Y (2006): A PID model of human balance keeping. *IEEE Control Systems Magazine.* 26:18–23.
7. Mergner T (2007): Modeling sensorimotor control of human upright stance In: Cisek P, Drew T, Kalaska JF, editors. *Progress in Brain Research: Elsevier*, pp 283–297.
8. Jian J (2018): *Modeling of Human Motor Control and Its Application in Human Interaction with Machines: University of Pittsburgh.*
9. Koiwai K, Liao Y, Yamamoto T, Nanjo T, Yamazaki Y, Fujimoto Y (2016): Human Skill Evaluation Based on Control Engineering Approach. *IFAC-PapersOnLine.* 49:633–638.
10. Insel T, Cuthbert B, Garvey M, Heinssen R, Pine DS, Quinn K, et al. (2010): Research domain criteria (RDoC): toward a new classification framework for research on mental disorders. *Am J Psychiatry.* 167:748–751. [PubMed: 20595427]
11. Watson D, Stanton K, Clark LA (2017): Self-report indicators of negative valence constructs within the research domain criteria (RDoC): A critical review. *J Affect Disord.* 216:58–69. [PubMed: 27823854]
12. McTeague LM, Lang PJ (2012): The anxiety spectrum and the reflex physiology of defense: from circumscribed fear to broad distress. *Depress Anxiety.* 29:264–281. [PubMed: 22511362]
13. National Institute of Mental Health (2011): *Negative valence systems: workshop proceedings.*
14. Sharp PB, Miller GA, Heller W (2015): Transdiagnostic dimensions of anxiety: Neural mechanisms, executive functions, and new directions. *Int J Psychophysiol.* 98:365–377. [PubMed: 26156938]
15. National Institute of Mental Health (2019): *Sensorimotor Domain Added to the RDoC Framework.*
16. Huang H, Harle K, Movellan J, Paulus M (2016): Using Optimal Control to Disambiguate the Effect of Depression on Sensorimotor, Motivational and Goal-Setting Functions. *PLoS One.* 11:e0167960. [PubMed: 27973592]
17. Milad MR, Quirk GJ, Pitman RK, Orr SP, Fischl B, Rauch SL (2007): A role for the human dorsal anterior cingulate cortex in fear expression. *Biol Psychiatry.* 62:1191–1194. [PubMed: 17707349]
18. Paus T (2001): Primate anterior cingulate cortex: where motor control, drive and cognition interface. *NatRevNeurosci.* 2:417–424.
19. Kroencke K, Spitzer R, Williams J (2001): The PHQ-9: validity of a brief depression severity measure. *Journal of General Internal Medicine.* 16:606–613. [PubMed: 11556941]
20. Campbell-Sills L, Norman SB, Craske MG, Sullivan G, Lang AJ, Chavira DA, et al. (2009): Validation of a brief measure of anxiety-related severity and impairment: the Overall Anxiety Severity and Impairment Scale (OASIS). *Journal of affective disorders.* 112:92–101. [PubMed: 18486238]
21. Sheehan DV, Lecrubier Y, Sheehan KH, Amorim P, Janavs J, Weiller E, et al. (1998): The Mini-International Neuropsychiatric Interview (MINI): the development and validation of a structured diagnostic psychiatric interview for DSM-IV and ICD-10. *Journal of clinical psychiatry.* 59:22–33.
22. Watson D, Clark LA (1999): *The PANAS-X: Manual for the positive and negative affect schedule-expanded form.*
23. Stan Development Team (2018): *RStan: the R interface to Stan.*

24. Carpenter B, Gelman A, Hoffman MD, Lee D, Goodrich B, Betancourt M, et al. (2017): Stan: A Probabilistic Programming Language Journal of Statistical Software. Medium: ED; Size: 32 p.
25. Barlow DH (2000): Unraveling the mysteries of anxiety and its disorders from the perspective of emotion theory. *Am Psychol.* 55:1247–1263. [PubMed: 11280938]
26. Pine DS (2017): Clinical Advances From a Computational Approach to Anxiety. *Biol Psychiatry.* 82:385–387. [PubMed: 27836100]
27. Bach DR (2015): Anxiety-Like Behavioural Inhibition Is Normative under Environmental Threat-Reward Correlations. *PLoS Comput Biol.* 11:e1004646. [PubMed: 26650585]
28. Korn CW, Vunder J, Miro J, Fuentemilla L, Hurlemann R, Bach DR (2017): Amygdala Lesions Reduce Anxiety-like Behavior in a Human Benzodiazepine-Sensitive Approach-Avoidance Conflict Test. *Biol Psychiatry.* 82:522–531. [PubMed: 28364943]
29. Browning M, Behrens TE, Jocham G, O'Reilly JX, Bishop SJ (2015): Anxious individuals have difficulty learning the causal statistics of aversive environments. *Nat Neurosci.* 18:590–596. [PubMed: 25730669]
30. Huang H, Thompson W, Paulus MP (2017): Computational Dysfunctions in Anxiety: Failure to Differentiate Signal From Noise. *Biol Psychiatry.* 82:440–446. [PubMed: 28838468]
31. Aupperle RL, Paulus MP (2010): Neural systems underlying approach and avoidance in anxiety disorders. *Dialogues Clin Neurosci.* 12:517–531. [PubMed: 21319496]
32. Todorov E (2004): Optimality principles in sensorimotor control. *Nat Neurosci.* 7:907–915. [PubMed: 15332089]
33. Kirk DE (2004): *Optimal Control Theory: An Introduction.* Dover Publications.
34. Enkavi AZ, Eisenberg IW, Bissett PG, Mazza GL, MacKinnon DP, Marsch LA, et al. (2019): Large-scale analysis of test-retest reliabilities of self-regulation measures. *Proc Natl Acad Sci U S A.* 116:5472–5477. [PubMed: 30842284]
35. Hedge C, Powell G, Sumner P (2018): The reliability paradox: Why robust cognitive tasks do not produce reliable individual differences. *Behav Res Methods.* 50:1166–1186. [PubMed: 28726177]
36. Boehm U, Marsman M, Matzke D, Wagenmakers EJ (2018): On the importance of avoiding shortcuts in applying cognitive models to hierarchical data. *Behav Res Methods.* 50:1614–1631. [PubMed: 29949071]
37. Rouder JN, Kumar A, Haaf JM (2019): Why Most Studies of Individual Differences With Inhibition Tasks Are Bound To Fail. *PsyArXiv.*
38. Scott SH (2012): The computational and neural basis of voluntary motor control and planning. *Trends Cogn Sci.* 16:541–549. [PubMed: 23031541]

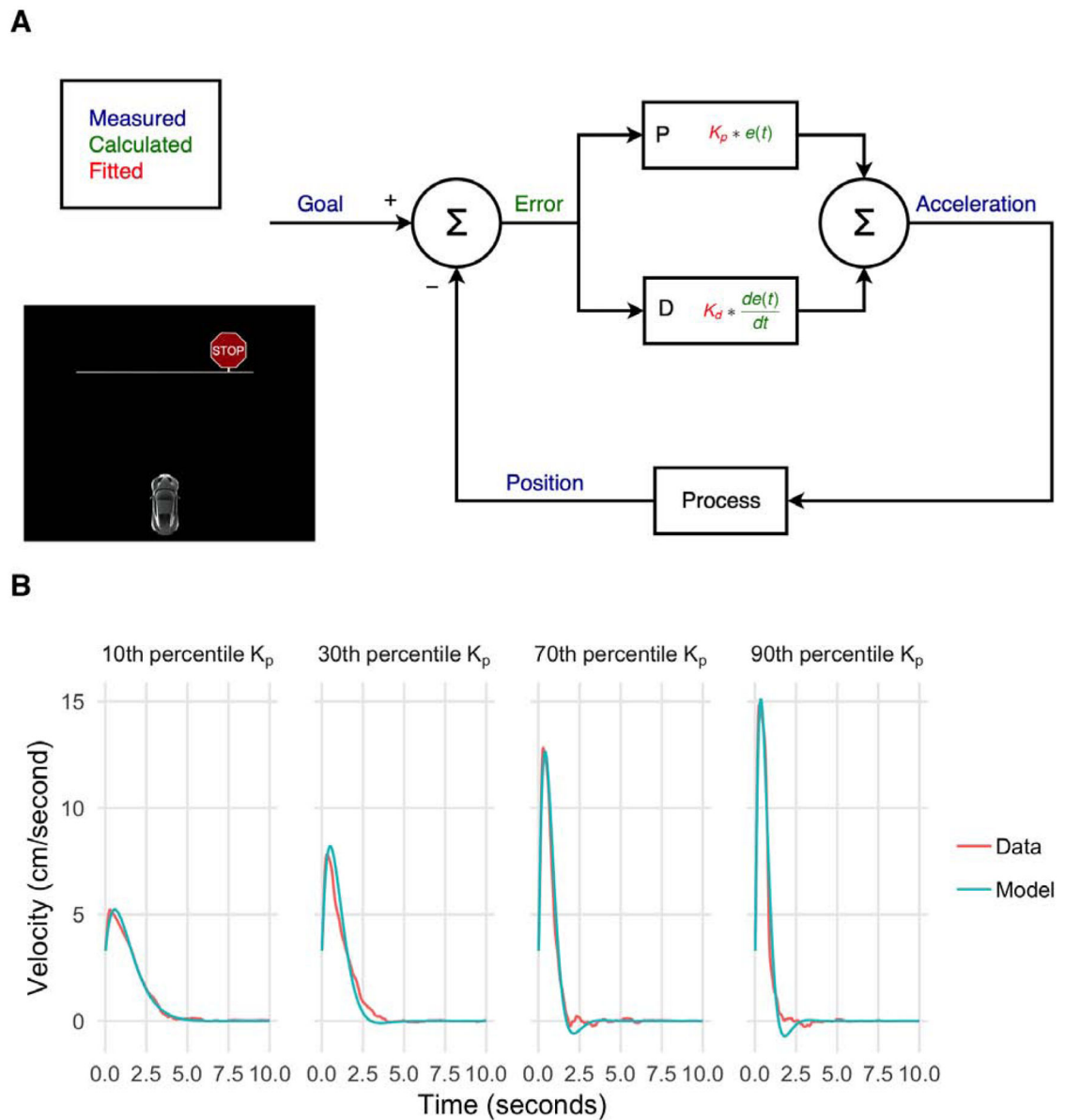


**Figure 1:**

Proportion-derivative (PD) control model of a virtual driving task.

(a) PD control framework. At each timepoint, error is calculated by subtracting the current position from the goal position. The control action (i.e. acceleration) at each timepoint is a linear combination of the current error and derivative of the error, with coefficients  $K_p$  and  $K_d$ , respectively. Goal state is taken to be the final position of the car at the end of the trial. Goal state, current position, and acceleration are directly measured during the task, whereas current error and derivative of the error are calculated based on these quantities, and  $K_p$  and  $K_d$  are determined based on a hierarchical model-fitting process. The virtual driving task is shown as an inset in the figure.

(b) Example model fits for four subjects. Subjects were chosen based on fitted  $K_p$  (10<sup>th</sup> percentile, 30<sup>th</sup> percentile, 70<sup>th</sup> percentile, and 90<sup>th</sup> percentile) to illustrate a range of

different behaviors on the task. The red traces (data traces) show mean velocity at each time point across all trials for each subject. The green traces (simulation traces) were generated via autonomous simulations using the forward PD model from starting conditions, using the fitted mean  $K_p$  and  $K_d$  for each subject.

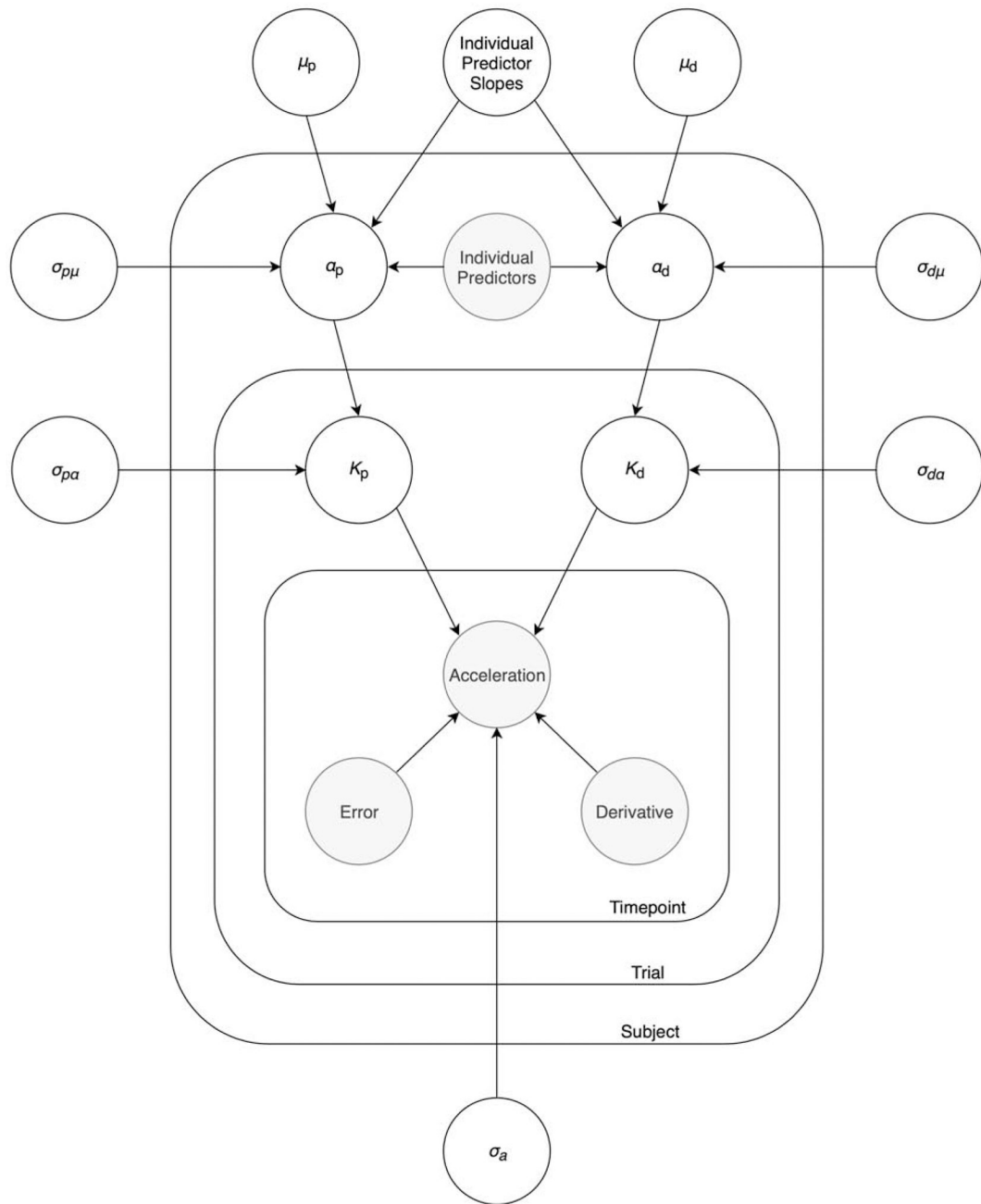


**Figure 2:** Hierarchical Bayesian model. The graphical model depicts the hierarchical PD control modeling approach. Shaded circles represent data, while non-shaded circles represent parameters. At each timepoint within a trial, acceleration depends on error and derivative of the error according to the PD control model.  $K_p$  and  $K_d$  for each trial represent the coefficients of the error term and derivative term, respectively. Trial-level  $K_p$  and  $K_d$  are drawn from subject-level means ( $\alpha_p$  and  $\alpha_d$ ), which themselves are drawn from group-level means ( $\mu_p$ , and  $\mu_d$ ). Depending on the particular model,  $\alpha_p$  and  $\alpha_d$  can be related to individual-level predictors such as self-report scores, demographics, and brain region



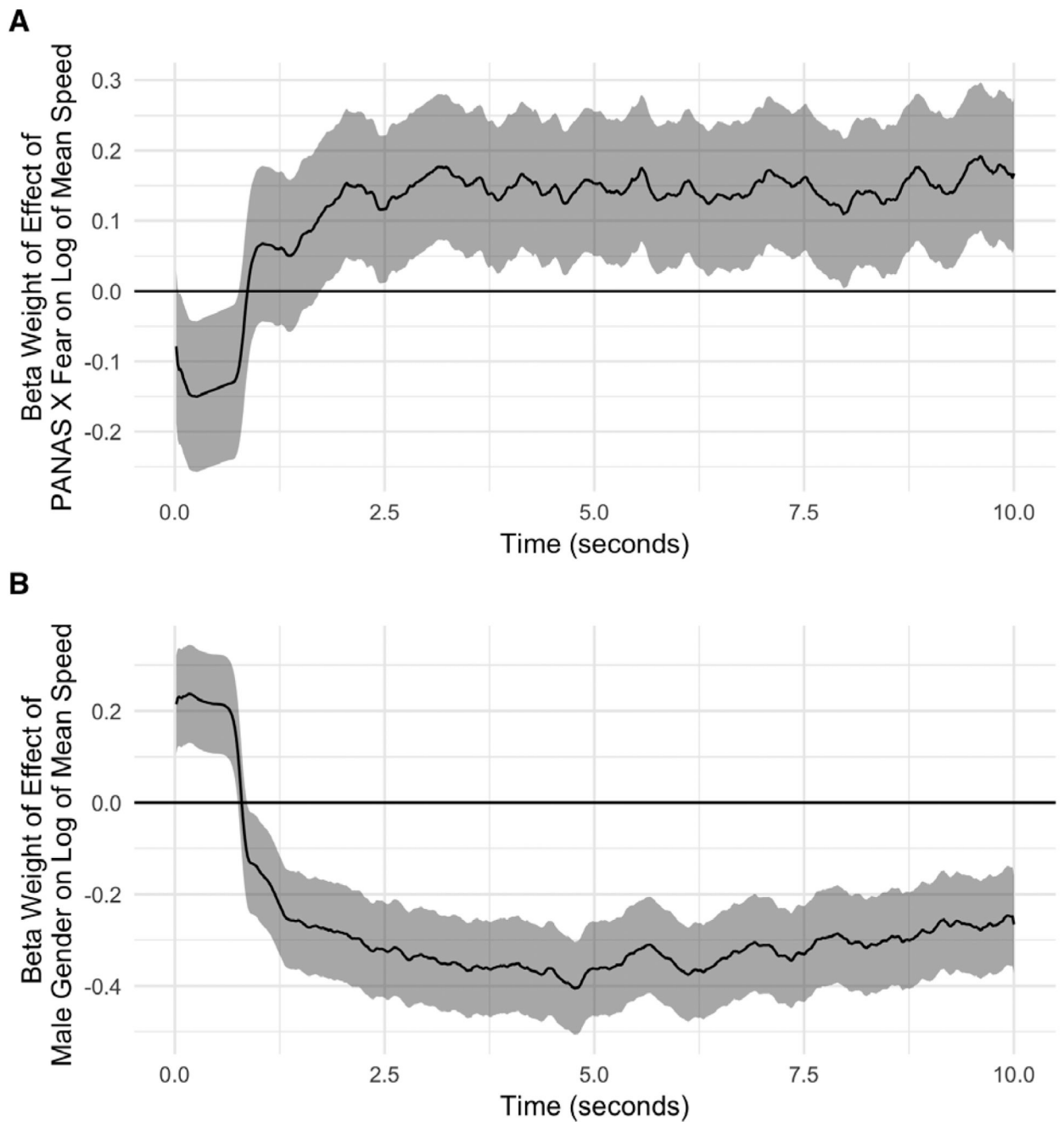
volumes. The  $\sigma$  terms represent standard deviations. See Methods section for details of the modeling approach.

Author Manuscript

Author Manuscript

Author Manuscript

Author Manuscript

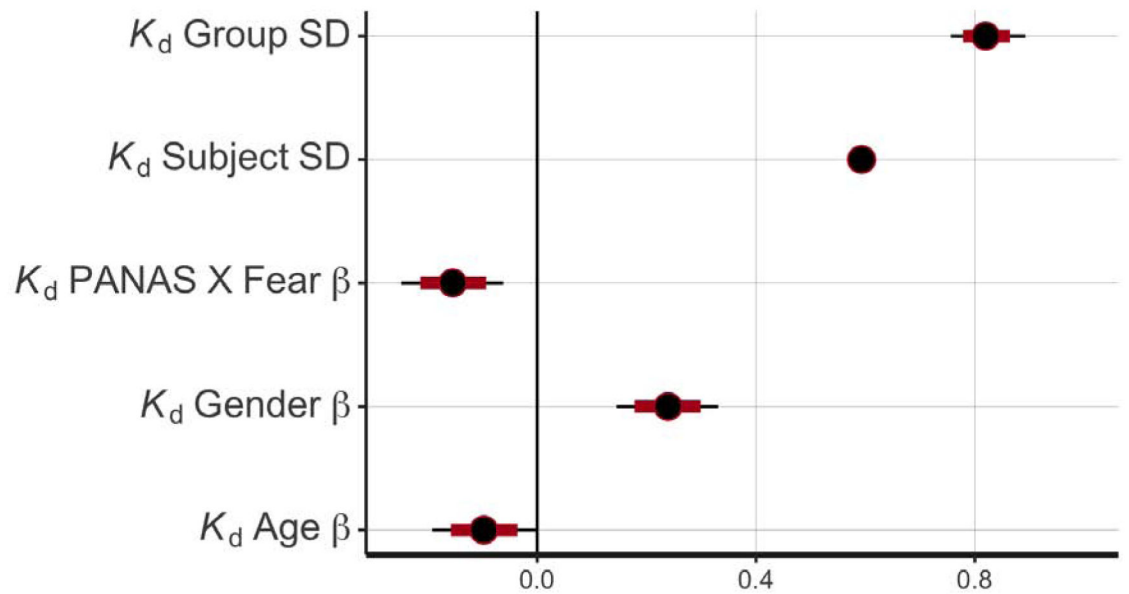
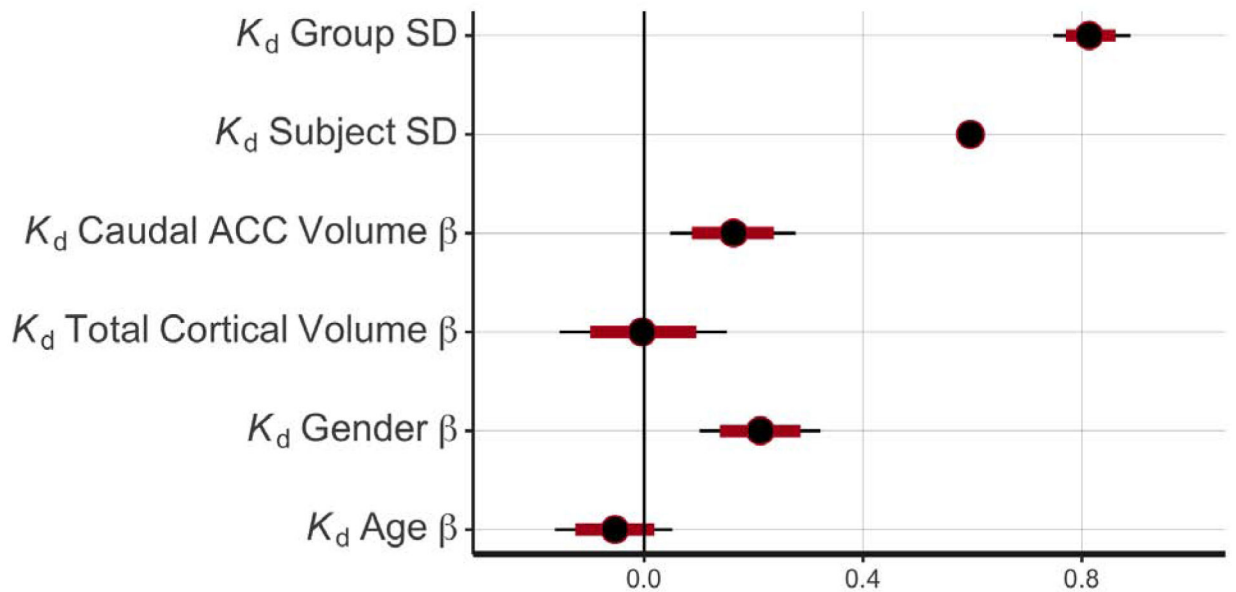


**Figure 3:**  
Behavioral results.

(a) Relationship between PANAS X Fear score and log of mean speed throughout the course of the trial. Log of mean speed captures both rise time (speed of reaching the goal early in the trial) and settling time (decay of oscillations later in the trial). The beta weight (i.e. standardized regression coefficient) for the relationship between PANAS X Fear score and log of mean speed, controlling for gender and age, is shown for each time point over the course of the 10-second trial, with shaded regions representing 95% confidence intervals.

Fearful subjects displayed lower log mean speed early in the trial and higher log mean speed later in the trial, consistent with slower rise time and longer settling time.

(b) Relationship between male gender and log of mean speed throughout the course of the trial. The beta weight (i.e. standardized regression coefficient) for the relationship between gender and log of mean speed, controlling for age, is shown for each time point over the course of the 10-second trial, with shaded regions representing 95% confidence intervals. Male subjects displayed higher log mean speed early in the trial and lower log mean speed later in the trial, consistent with faster rise time and shorter settling time.

**A****B****Figure 4:**

Relationships between  $K_d$  and individual-level predictors.

(a) Relationship between  $K_d$  (damping) parameter and PANAS X Fear score, controlling for gender and age. The hierarchical model additionally included relationships between the  $K_p$  (driving) parameter and the same individual-level predictors (see Supplementary Figure S7a). For each parameter, the median of the posterior distribution (black circle), 80% credible interval (red line), and 95% credible interval (black line) are shown. Individual-level predictors (i.e. PANAS X Fear score, gender, and age) were scaled (i.e. z-scored) prior to model-fitting. PANAS X Fear score was negatively associated with  $K_d$ .

(b) Relationship between  $K_d$  (damping) parameter and caudal ACC volume, controlling for total cortical volume, gender and age. The hierarchical model additionally included relationships between the  $K_p$  (driving) parameter and the same individual-level predictors (see Supplementary Figure S7a). Individual-level predictors were scaled (i.e. z-scored) prior to model-fitting. Caudal ACC volume was positively associated with  $K_d$ .